

Spirohydantoin derivatives of thiopyrano[2,3-*b*]pyridin-4(4*H*)-one as potent in vitro and in vivo aldose reductase inhibitors

Federico Da Settimo,^{a,*} Giampaolo Primofiore,^a Concettina La Motta,^a
Silvia Salerno,^a Ettore Novellino,^b Giovanni Greco,^b Antonio Lavecchia,^b
Sonia Laneri^b and Enrico Boldrini^c

^a*Dipartimento di Scienze Farmaceutiche, Università di Pisa, Via Bonanno 6, 56126 Pisa, Italy*

^b*Dipartimento di Chimica Farmaceutica e Tossicologica, Università di Napoli 'Federico II', Via Domenico Montesano, 49, 80131 Napoli, Italy*

^c*Opocrin S.p.A., Via Pacinotti 3, 41040 Corlo di Formigine (Modena), Italy*

Received 25 May 2004; accepted 5 October 2004

Available online 2 November 2004

Abstract—The 2,3-dihydrospiro[4*H*-thiopyrano[2,3-*b*]pyridin-4,4'-imidazolidine]-2',5'-dione **3** and its 7-methyl analogue **4** were synthesized and tested for their ability to inhibit aldose reductase (ALR2). To expand the structure–activity relationships, the sulfone **5** and the acetic acid derivative **7** were also prepared and tested. Compounds **3** and **4** proved to be potent ALR2 inhibitors, with IC₅₀ values in the submicromolar range (0.96 and 0.94 μM, respectively) similar to that of sorbinil (0.65 μM). Moreover, compound **3** was found to be highly potent in preventing cataract development in severely galactosemic rats, like tolrestat, when administered as an eyedrop solution. Docking simulations of both *R*- and *S*-isomers of **3** into the ALR2 crystal structure were carried out to guide, prospectively, the design of new analogues.

© 2004 Elsevier Ltd. All rights reserved.

1. Introduction

Diabetic hyperglycemia causes a marked increase in glucose metabolism through the polyol pathway in those tissues in which glucose transport is insulin-independent. The correlation existing between enhanced polyol pathway glucose metabolism and the onset and progression of long-term diabetic complications such as neuropathy, retinopathy, nephropathy and cataract has been well documented. Aldose reductase (alditol:NADP⁺ oxidoreductase, EC 1.1.1.21 ALR2), a member of the aldo–keto reductase superfamily, is the first enzyme of the polyol pathway, which catalyzes the NADPH-dependent reduction of excess glucose to sorbitol. In this way, the concentration of sorbitol increases markedly, and its accumulation has been linked to cellular damage leading to the diabetic complications. Consequently, inhibitors of ALR2 (ARIs) have received attention as possible therapeutic drugs, seeing that they can safely

prevent or stop the progression of these long-term complications, with no risk of hypoglycemia, since they have no effect on plasma glucose levels.^{1–5}

Among the numerous structurally different compounds, which reportedly inhibit ALR2, the most potent classes are the spirohydantoin derivatives, such as sorbinil (Chart 1), and the acetic acid compounds, which include alrestatin, tolrestat, zopolrestat and epalrestat (Chart 1). Unfortunately, only the last of these is on the market nowadays, since ARI-based therapy suffers from many limitations due to pharmacokinetic problems, reversibility of diabetic neuropathy, adverse reactions and poor reproducibility of clinical measurements.^{3–6}

For several years our group has been interested in the search for highly potent ARIs able to prevent cataract development (severely galactosemic rat model) by topical administration,^{7,8} thus avoiding bioavailability and/or metabolism-related problems associated with systemic administration. Actually, tolrestat has been reported to be highly potent in preventing sugar cataract formation when topically administered to rats fed with 50% galactose diet.⁹

Keywords: Aldose reductase; Inhibitors; Spirohydantoin derivatives; Cataract.

*Corresponding author. Tel.: +39 050 2219547; fax: +39 050 2219605; e-mail: fsettimo@farm.unipi.it

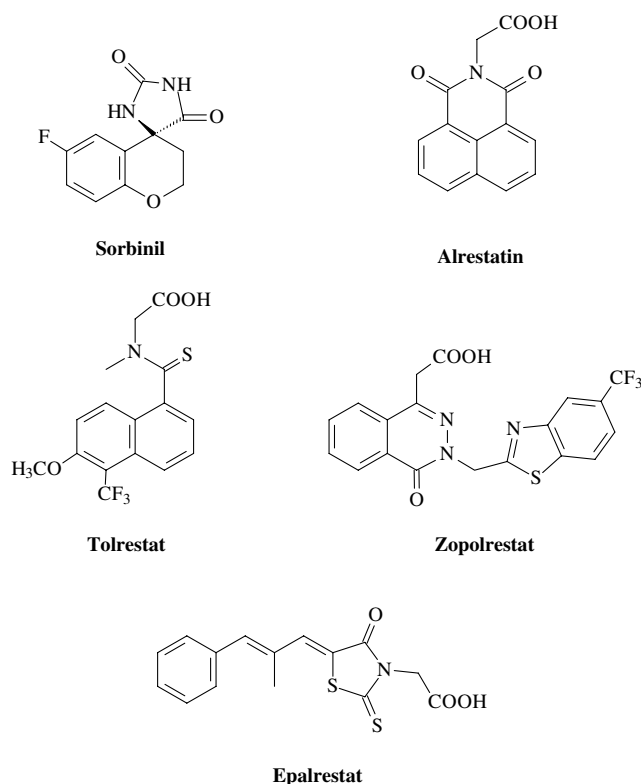


Chart 1.

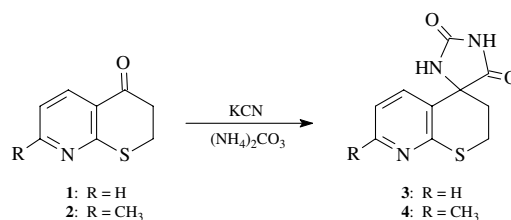
In the course of our drug discovery programs, we were intrigued by the structure–activity relationships described by Sarges and co-workers for spirohydanthione derivatives. Firstly, this author reports that a good inhibitory potency is maintained by sorbinil-like compounds in which the oxygen atom of the pyrane ring is substituted by a sulfur atom.¹⁰ In a subsequent paper, the same author reports that 8-aza analogues of sorbinil are more potent in vitro and in vivo inhibitors than the parent compound.¹¹ This experimental evidence, combined with our previous experience in the synthesis of ketones 2,3-dihydrothiopyrano[2,3-*b*]pyridin-4(4*H*)-one **1** and its 7-methyl analogue **2**,^{12–14} led us to synthesize and test for their ALR2 inhibitory activity the spirohy-

dantoin derivatives of **1** and **2**, namely **3** and **4**. A preliminary overlay of the molecular models of both *R*- and *S*-isomers of **3** on the ALR2-bound conformation of sorbinil¹⁵ gave support to our project, because it showed a satisfactory match of the common spirohydanthione ring and the benzopyrane/pyrano[2,3-*b*]pyridine systems (Fig. 1): the overlay of *S*-**3** on sorbinil is remarkable yielding a root-mean-square (rms) deviation of 0.03 Å. For *R*-**3** the departure from direct superimposition is greater (rms 0.74 Å), but still acceptable. In order to delineate better the structure–activity relationships (SARs) of this new class of ARIs, the sulfone **5** and the acetic acid derivative **7** were also prepared and tested.

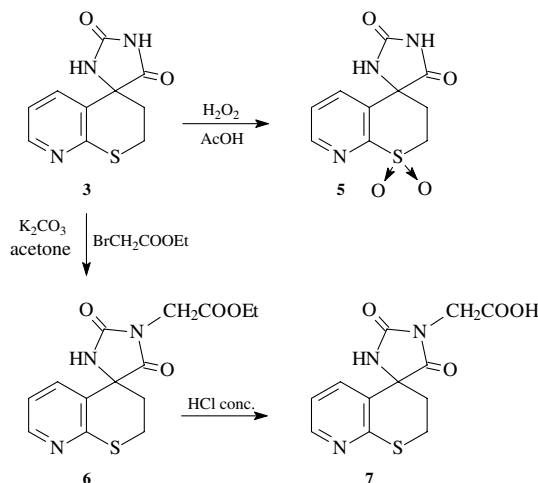
2. Chemistry

Spirohydanthiones **3** and **4** were synthesized, as shown in Scheme 1, by reaction of the corresponding ketone precursors, **1** and **2**, with KCN and powered $(\text{NH}_4)_2\text{CO}_3$ in aqueous ethanol (50% v/v) at 50 °C for 24 h, under standard Bucherer–Berg conditions.¹⁶

Sulfone **5** was obtained with a 58% yield by treatment of spirohydanthione **3** with 30% hydrogen peroxide in acetic acid at 80 °C (Scheme 2). Acetic acid derivative **7** was prepared in two steps. Alkylation of **3** with ethyl bromoacetate in refluxing acetone, in the presence of anhydrous potassium carbonate, gave the ethyl ester



Scheme 1.



Scheme 2.

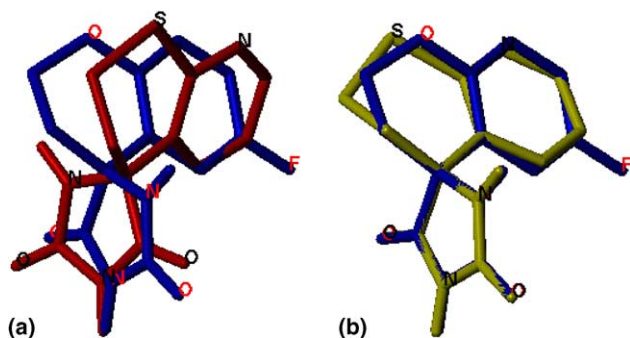


Figure 1. Overlay of (a) *R*-isomer (red) and (b) *S*-isomer (yellow) of **3** on the experimentally determined ALR2-bound conformation of sorbinil (blue) by minimizing the root-mean-square distance between the benzo-fused ring centroids and the common CO–NH–CO spirohydanthione moiety.

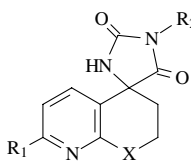
intermediate **6**, which was then hydrolyzed in an aqueous sodium hydroxide solution to give the target compound **7**.

All the newly synthesized spirohydantoin derivatives **3–7** were obtained and characterized as racemic mixtures (Table 1).

3. Biochemistry and pharmacology

Compounds **3–5** and **7** were evaluated for their in vitro inhibitory activity against ALR2, carrying out the screening on a water-soluble enzymatic extract purified from rat lenses.^{17–20} IC₅₀ values were determined by

Table 1. Physical properties and spectral data of spirohydantoin derivatives **3–7**

|  | | | | | | | | | | |
|---|-----------------|-----------------|-----------------------|-----------|------------------------------|---|--|---|------------------------------------|--|
| No. | X | R ₁ | R ₂ | Yield (%) | Mp (°C) recryst solv | Formula ^a | IR (ν, cm ⁻¹) | NMR (δ, ppm) | MS (<i>m/e</i>) | |
| 3 | S | H | H | 60 | >300 EtOH | C ₁₀ H ₉ N ₃ O ₂ S | 3330, 3250, 3225, 1770, 1700 | 2.21–2.35 (m, 2H, CH ₂), 3.13–3.43 (m, 2H, SCH ₂), 7.08 (dd, 1H, H ₆), 7.49 (d, 1H, H ₅), 8.28 (d, 1H, H ₇), 8.54 (s, 1H, CONH, exc), 10.94 (s, 1H, CONHCO, exc) | 235 [M ⁺], 136 base | |
| 4 | S | CH ₃ | H | 52 | 280–282 EtOH | C ₁₁ H ₁₁ N ₃ O ₂ S | 3330, 3250, 3225, 1770, 1700 | 2.20–2.28 (m, 2H, CH ₂), 2.36 (s, 3H, CH ₃), 3.08–3.40 (m, 2H, SCH ₂), 6.97 (d, 1H, H ₆), 7.38 (d, 1H, H ₅), 8.61 (s, 1H, CONH, exc), 11.03 (s, 1H, CONHCO, exc) | 249 [M ⁺], 43 base | |
| 5 | SO ₂ | H | H | 58 | >300 EtOH | C ₁₀ H ₉ N ₃ O ₄ S | 3340, 3270, 3063, 1780, 1703 | 2.48–2.78 (m, 2H, CH ₂), 3.73–4.00 (m, 2H, SCH ₂), 7.74 (dd, 1H, H ₆), 7.81 (d, 1H, H ₅), 8.77–8.80 (m, 2H, H ₇ , CONH), 10.94 (s, 1H, CONHCO, exc) | 267 [M ⁺], 104 base | |
| 6 | S | H | CH ₂ COOEt | 79 | 107–108 EtOH | C ₁₄ H ₁₅ N ₃ O ₄ S | 3650, 3100, 1780, 1760, 1720 | 1.21 (t, 3H, CH ₃), 2.27–2.49 (m, 2H, CH ₂), 3.24–3.30 (m, 4H, SCH ₂ , OCH ₂), 4.27 (s, 2H, CH ₂ CO), 7.17 (dd, 1H, H ₆), 7.61 (d, 1H, H ₅), 8.35 (d, 1H, H ₇), 9.21 (s, 1H, NH, exc) | 321 [M ⁺], 136 base | |
| 7 | S | H | CH ₂ COOH | 89 | 245–248 ^t PrOH | C ₁₂ H ₁₁ N ₃ O ₄ S | 3490, 3077, 1774, 1746, 1710, 1639 | 2.25–2.51 (m, 2H, CH ₂), 3.15–3.40 (m, 2H, SCH ₂), 4.16 (s, 2H, CH ₂ CO), 7.15 (dd, 1H, H ₆), 7.63 (d, 1H, H ₅), 8.35 (d, 1H, H ₇), 9.16 (s, 1H, NH, exc), 13.15 (br s, 1H, COOH, exc) | 293 [M ⁺], 45 base | |

^a Elemental analyses were within ±0.4% of the calculated values.

Table 2. Enzyme inhibition data of spirohydantoin 3–5 and 7

| No. | Aldose reductase IC ₅₀ ^a (μM) | Aldehyde reductase IC ₅₀ ^a (μM) | Sorbitol dehydrogenase IC ₅₀ ^a (μM) | Glutathione reductase IC ₅₀ ^a (μM) |
|-----------|--|--|--|---|
| 3 | 0.96 (0.92–1.01) | 3.40 (3.26–3.55) | n.a. ^b | n.a. |
| 4 | 0.94 (0.89–0.99) | 1.11 (1.05–1.19) | n.a. | n.a. |
| 5 | 4.50 (4.43–4.57) | 1.36 (1.29–1.43) | n.a. | n.a. |
| 7 | 8.90 (8.54–9.26) | 50.0 (47.30–52.70) | n.a. | n.a. |
| Sorbinil | 0.65 (0.49–0.82) | 0.029 (0.020–0.038) | n.a. | n.a. |
| Tolrestat | 0.05 (0.03–0.06) | n.a. | n.a. | n.a. |
| Quercetin | 7.81 (5.47–10.15) | 2.32 (2.05–2.78) | 35.6 (31.6–40.0) | 48.8 (34.7–63.4) |

^a IC₅₀ values represent the concentration required to produce 50% enzyme inhibition.

^b n.a. = not active.

linear regression analysis of the log concentration–response curve. As one of the most important requirements of clinically useful ARIs is their ALR2-selectivity over closely related enzymes, compounds **3–5** and **7** were also assayed for their ability to inhibit sorbitol dehydrogenase (SD)²¹ and two other enzymes not involved in the polyol pathway, namely aldehyde reductase (ALR1)²² and glutathione reductase (GR).²³ Sorbinil,²⁴ tolrestat²⁵ and quercetin²⁶ were used as the reference standards.

Compound **3** was investigated in vivo for its ability to prevent cataract development in severely galactosemic rats.²⁴ Its effectiveness was evaluated with respect to tolrestat as a highly potent reversible inhibitor of lenticular ALR2 when topically administered to rats fed with 50% galactose diet.⁹

4. Results and discussion

Spirohydantoin derivatives **3** and **4** proved to be potent ALR2 inhibitors, with IC₅₀ values in the submicromolar range (0.96 and 0.94 μM, respectively) similar to that of sorbinil (0.65 μM), and one order of magnitude higher than that of tolrestat (0.05 μM) (Table 2).

The oxidation of the sulfur atom of **3** to give **5** (IC₅₀ 4.5 μM) determined a 5-fold lowering in potency; likewise, the introduction of an acetic residue at the N(1') of **3**, as in **7** (IC₅₀ 8.90 μM), was detrimental for the activity. Like sorbinil, compounds **3–5** and **7** also proved to inhibit ALR1, but none of them displayed any appreciable inhibitory property towards SD or GR.

Compound **3** was administered as an eyedrop solution in the precorneal region to investigate its in vivo ability to prevent cataract development in severely galactosemic rats.^{7,8} Topical administration can in principle achieve significant drug levels in the lens with negligible effects on other tissues, thus avoiding bioavailability and/or metabolism-related problems associated with systemic administration.⁹ The pharmacological data are reported in Table 3. After 21 days of a 50% galactose diet, 90% of the animals treated only with the vehicle developed nuclear cataract. Those treated with 1% ophthalmic solution of **3** were only partially protected, whereas those treated with 3% solution were 100% protected, as no nuclear cataract was detected in any rats.

Table 3. Effect of treatment with ophthalmic solution of **3** and tolrestat on development of nuclear cataract in severely galactosemic rats

| Day of treatment | Rats with nuclear cataract (%) | | | | |
|------------------|--------------------------------|------------------|------------------|-------------------|-------------------|
| | Control | 3 (1%) | 3 (3%) | Tolrestat (1%) | Tolrestat (3%) |
| 11 | 13 | 0 | 0 | 0 | 0 |
| 12 | 25 | 5 | 0 | 0 | 0 |
| 13 | 25 | 5 | 0 | 0 | 0 |
| 14 | 25 | 5 | 0 | 23 | 0 |
| 15 | 25 | 15 | 0 | 32 | 0 |
| 16 | 31 | 15 | 0 | 32 | 0 |
| 17 | 50 | 35 | 0 | 32 | 0 |
| 18 | 50 | 35 | 0 | 43 | 0 |
| 19 | 75 | 48 | 0 | 43 | 0 |
| 20 | 88 | 48 | 0 | 47 | 0 |
| 21 | 90 | 60 | 0 | 47 | 0 |

Table 4. Physical properties of compound **3**, tolrestat and sorbinil

| | CLog <i>P</i> ^a | p <i>K</i> _a | PSA ^b (Å ²) |
|-----------|----------------------------|-------------------------|------------------------------------|
| 3 | −0.05 | 10.2 | 93.1 |
| Tolrestat | 3.72 | 2.64 | 71.8 |
| Sorbinil | 0.64 | 8.70 ^c | 69.3 |

^a Calculated *n*-octanol/water partition coefficient.³⁴

^b Polar surface area.³²

^c Data taken from Ref. 10.

In this assay, the protection trend exerted by compound **3** proved to be similar to that of tolrestat in both 1% and 3% solutions, in spite of a higher IC₅₀ value, but less effective than sorbinil, which is reported to completely protect galactosemic rats from cataract development with 1% ophthalmic solution.²⁴ These results can be well understood from an analysis of the corneal anatomy, and the physical properties of compound **3**, tolrestat and sorbinil (Table 4). The cornea is formed by three primary layers: epithelium, stroma and endothelium. Both the epithelium and the endothelium are lipophilic and constitute the main barriers to hydrophilic compounds. The stroma is an aqueous layer and limits the movement of lipophilic compounds across the cornea. Thus, a compound usually has greater corneal permeability when its hydrophilic–lipophilic properties are adequately balanced. Compound **3** and tolrestat are less active than sorbinil, and show the same trend of in vivo potency although they present different physical properties (Table 4). Actually, compound **3** is less lipophilic,

but it is also fairly polar and less ionized with respect to tolrestat, which is more lipophilic, less polar, but also more acid. Thus, in both compounds the effects of lipophilicity/polarity/ionization are adequately counterbalanced to permeate the cornea. Sorbinil is the most in vivo active compound, since it displays the best balance between lipophilicity and polarity/ionization as evidenced by its values of Clog*P*, PSA and p*K*_a, respectively (Table 4).

Docking simulations of **3** into the ALR2 binding site were carried out in order to propose a binding mode of these types of inhibitors at the enzyme catalytic site, which might be useful for the prospective design of new analogues. As all the tested compounds were assayed as racemic mixtures, we docked both *S*- and *R*-isomers of the inhibitor into the active site of the enzyme with the help of the program FlexX,²⁷ using the crystallographic coordinates of pig ALR2 complexed with sorbinil¹⁵ as a reference (filed in the Brookhaven Protein Data Bank²⁸ under the entry code 1AH3). Although the inhibition assays on our compounds were conducted on rat ALR2, the use of a model of pig ALR2 for docking studies is justified by the following facts: (i) the crystal

structure of rat ALR2 is unknown; (ii) the pig and rat sequences of this enzyme are characterized by 81% identity and 87% homology;²⁹ (iii) all active-site residues, including those of the specificity pocket, are largely conserved across the ALR2 isoforms so far sequenced.¹⁵

The energy-minimized structure of sorbinil was preliminarily docked into ALR2 to examine how closely the FlexX algorithm can reproduce the experimentally determined binding conformation of sorbinil at the active site of ALR2.¹⁵ A superposition of docked sorbinil onto the crystallographic geometry yielded an rms deviation of 0.74 Å, thus revealing that FlexX was successful in reproducing the binding conformation of sorbinil.

The free binding energy of a protein–ligand complex is estimated in FlexX as the sum of free energy contributions from hydrogen bonds, ion-pair interactions, hydrophobic and π -stacking interactions of aromatic groups and lipophilic interactions. The docking results (highest-scoring binding modes) for both *R*- and *S*-isomers of **3** in ALR2 were calculated and showed free

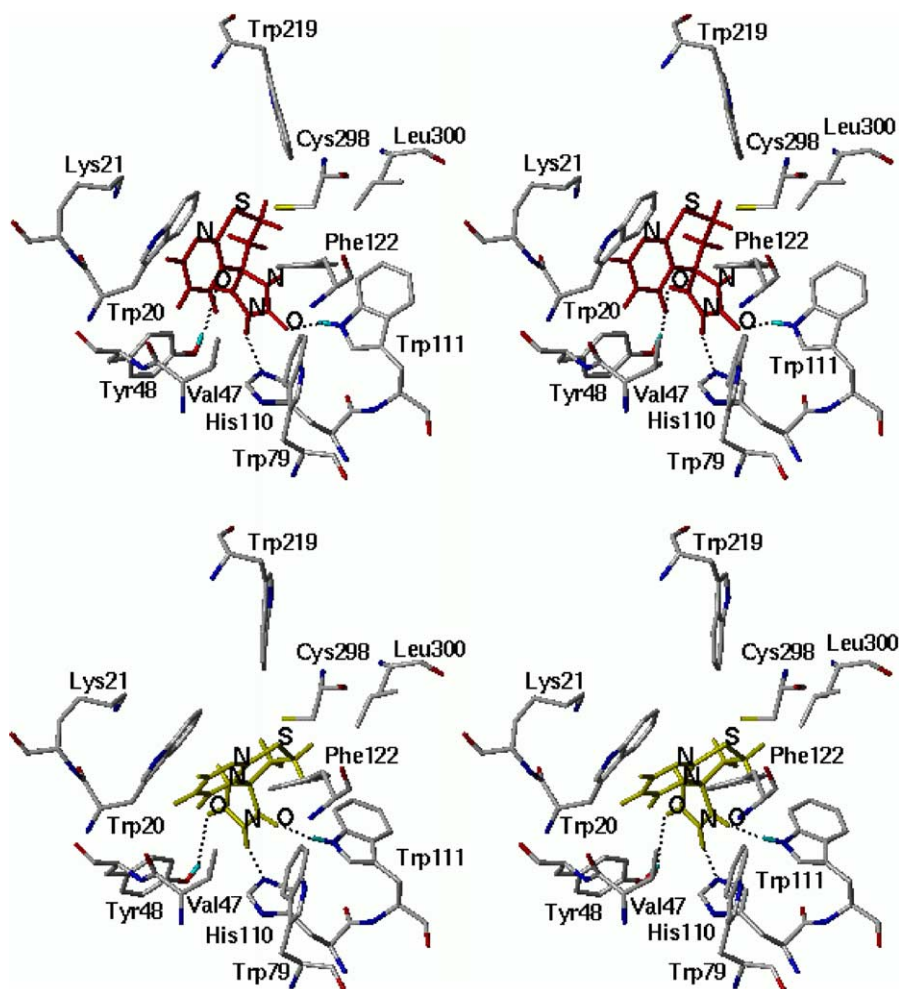


Figure 2. (*R*)-**3** (top) and (*S*)-**3** (bottom) isomers docked into the ALR2 binding site. Only aminoacids located within 5 Å distance of the bound ligand are displayed and labelled. The hydrogen bonds discussed in the text are depicted as black dashed lines.

binding energies of ΔG -4.0 kcal/mol and ΔG -3.7 kcal/mol, respectively. Taking into account the accuracy of the current docking methods, the binding free energies associated with the ALR2/*R*-**3** and ALR2/*S*-**3** complexes were not sufficiently dissimilar to conclude, which of the two complexes (isomers) was biologically more significant. Thus, both ALR2/*R*-**3** and ALR2/*S*-**3** complexes were analyzed as though the binding modes of the enantiomers of **3** had the same probability of occurrence.

The three-dimensional structure of the ALR2/*R*-**3** and ALR2/*S*-**3** complexes is shown in Figure 2, where only the aminoacids located within 5 Å of the inhibitor are displayed. The main features of the final docking model are schematically represented in Figure 3.

The thiopyranopyridine ring is surrounded by the side chains of Trp20, Val47, Trp79, Trp111, Phe122, Trp219, Cys298 and Leu300 by means of hydrophobic interactions. In addition to these, the two carbonyl groups of the spirohydantoin ring form hydrogen bonds with the enzyme by hydrophilic interactions, in a manner similar to that of the carboxyl groups of zopolrestat, tolrestat and alrestatin. The carbonyl group in the 2'-position forms one of the hydrogen bonds with the O η of Tyr48 (2.5 Å) and is close to the nicotinamide ring of the coenzyme. The other carbonyl group in the 5'-position accepts another hydrogen bond from the N ϵ 1 of Trp111 (1.9 Å). The 1'-position NH group in the hydantoin ring is involved in a hydrogen bond with the N ϵ 2 of His110 (1.9 Å). Other important features are van der Waals and hydrophobic interactions: the aromatic side chains of Trp20, Trp79 and Phe122 are positioned to sandwich the thiopyranopyridine framework.

The crystal structure of sorbinil complexed with ALR2, presented by Urzhumtsev et al.,¹⁵ shows that the spirohydantoin ring binds in the so-called anionic binding

site, like the carboxylate moiety of zopolrestat,³⁰ and the benzopyrane system interacts favourably with Trp20. Similarly, our docking model places the spirohydantoin moiety of our inhibitors in the same oxyanion hole, and the thiopyranopyridine ring establishes a hydrophobic interaction with Trp20 (Fig. 2).

From the docking model illustrated in Figure 2, it may be also deduced that the high ALR2 inhibitory activity of the 7-methyl derivative **4** is the consequence of a favourable hydrophobic interaction of the methyl group with the Val47, Trp20 and Phe122 side chains. The endocyclic sulfur does not appear to interact with any protein group. However, the oxidation of sulfide to sulfone (compound **5**) places the two oxygens in an apolar environment, where the energy penalty for desolvation is detrimental for activity.

To understand the low ALR2 activity of **7**, this compound was docked into the ALR2 catalytic site. When the results of the docking of sorbinil and **7** were compared, the docking of **7** gave less favourable FlexX scores. Inspection of the docked structure indicated that the acetic residue at the N(1') of spirohydantoin pointed towards the entrance of the enzyme away from the catalytic binding site. Thus, we propose that the low activity of derivative **7** can be explained by the lack of favourable interactions between the acidic function of the ligand and the oxyanion hole, made up of His110, Trp111 and Tyr48 residues.

In conclusion, we have described the synthesis and the aldose reductase-inhibiting properties of a number of spirohydantoin derivatives of the versatile ketones 2,3-dihydrothiopyrano[2,3-*b*]pyridin-4(4*H*)-one **1** and its 7-methyl analogue **2**. Compounds **3** and **4** displayed the highest potency, with IC₅₀ values in the submicromolar range. Compound **3** also showed an excellent in vivo activity, as it completely protected severely galactosemic rats from the development of nuclear cataract in a manner quite similar to tolrestat. Docking experiments of both *R*- and *S*-isomers of **3** into the ALR2 binding site were performed to guide, prospectively, the design of new analogues.

5. Experimental protocols

5.1. Chemistry

Melting points were determined using a Reichert Kofler hot-stage apparatus and are uncorrected. IR spectra were recorded with a Pye Unicam Infracord Model PU956 in Nujol mulls. Routine ¹H NMR spectra were determined on a Varian Gemini 200 spectrometer using DMSO-*d*₆ as the solvent. Mass spectra were obtained on a Hewlett-Packard 5988 A spectrometer using a direct injection probe and an electron beam energy of 70 eV. Analytical TLC was carried out on Merck 0.2 mm pre-coated silica gel (60 F-254) aluminium sheets, with visualization by irradiation with a UV lamp. Elemental analyses were performed by our Analytical Laboratory and agreed with theoretical values to within $\pm 0.4\%$.

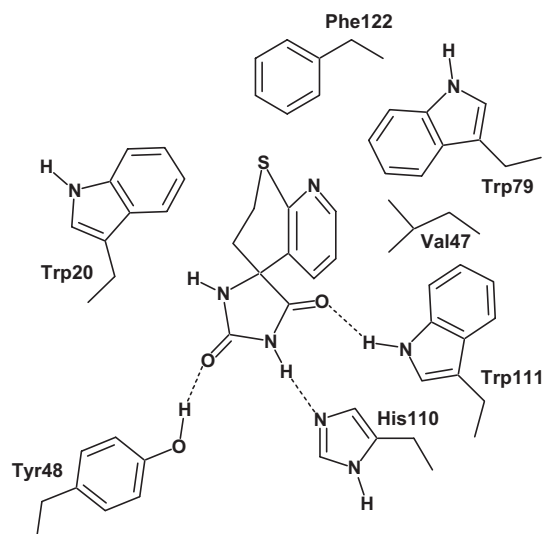


Figure 3. Schematic representation of the binding interactions (dashed lines) of inhibitor **3** at the active site of ALR2.

The ketone precursors 2,3-dihydrothiopyrano[2,3-*b*]pyridin-4(4*H*)-one¹² and 7-methyl-2,3-dihydrothiopyrano[2,3-*b*]pyridin-4(4*H*)-one¹³ were prepared in accordance with literature procedures.

5.1.1. 2,3-Dihydrospiro[4*H*-thiopyrano[2,3-*b*]pyridin-4,4'-imidazolidine]-2',5'-dione 3 and 2,3-dihydro-7-methylspiro[4*H*-thiopyrano[2,3-*b*]pyridin-4,4'-imidazolidine]-2',5'-dione 4. A suspension of ketone derivative 1 or 2 (1.00 mmol), KCN (0.098 g, 1.50 mmol) and powered (NH₄)₂CO₃ (0.288 g, 3.00 mmol) in 10 mL of 50% aqueous EtOH was heated at 50 °C for 24 h, until the disappearance of the starting material (TLC analyses). The reaction mixture was then diluted with 15 mL of water, boiled for 15 min, cooled to room temperature and acidified with concentrated HCl, under ice-cooling. The white solid precipitate was filtered, washed with water, dried and recrystallized (Table 1).

5.1.2. 2,3-Dihydrospiro[4*H*-thiopyrano[2,3-*b*]pyridin-4,4'-imidazolidine]-2',5'-dione-1,1-dioxide 5. A solution of spiro derivative 3 (0.235 g, 1.00 mmol) in 10 mL of acetic acid containing 2.5 mL of 30% H₂O₂ was heated under stirring at 80 °C for 20 h. After cooling and dilution with water, the white solid precipitate was filtered, dried and recrystallized (Table 1).

5.1.3. Ethyl 2,3-dihydrospiro[4*H*-thiopyrano[2,3-*b*]pyridin-4,4'-imidazolidine]-2',5'-dione-1'-ylacetate 6. A suspension of spiro derivative 3 (0.235 g, 1.00 mmol), ethyl bromoacetate (0.13 mL, 1.20 mmol) and anhydrous potassium carbonate (0.166 g, 1.20 mmol) in 5 mL of acetone was heated under reflux for 12 h. After cooling, the solid precipitate was collected, washed with water, dried and recrystallized (Table 1).

5.1.4. 2,3-Dihydrospiro[4*H*-thiopyrano[2,3-*b*]pyridin-4,4'-imidazolidine]-2',5'-dione-1'-ylacetic acid 7. A suspension of ester derivative 6 (0.320 g, 1.00 mmol) in 5 mL of 2% NaOH was left under stirring at room temperature for 15 h. The cloudy solution obtained was then filtered and acidified with concentrated HCl, under ice-cooling. The white solid precipitate was collected, washed with water, dried and recrystallized (Table 1).

5.2. Biology

5.2.1. Materials and methods. Aldose reductase (ALR2) and aldehyde reductase (ALR1) were obtained from Sprague Dawley albino rats, 120–140 g b.w., supplied by Harlan Nossan, Italy. In order to minimize cross-contamination between ALR2 and ALR1 in the enzyme preparation, rat lens, in which ALR2 is the predominant enzyme, and kidney, where ALR1 shows the highest concentration, were used for the isolation of ALR2 and ALR1, respectively.

Glutathione reductase (GR) type IV from bakers' yeast (100–300 U/mg), sorbitol dehydrogenase (SD) from sheep liver (10 U/mg of protein), pyridine coenzymes, D,L-glyceraldehyde, glutathione disulfide, sodium D-glucuronate, sorbitol and quercetin were from Sigma

Chemical Co. Sorbinil was a gift from Pfizer, Groton CT, USA. Tolrestat was obtained from Lorestat® Recordati, Italy. All other chemicals were of reagent grade.

5.2.2. Enzyme preparation

5.2.2.1. Aldose reductase (ALR2). A purified rat lens extract was prepared in accordance with the method of Hayman and Kinoshita³¹ with slight modifications. Lenses were quickly removed from rats following euthanasia and homogenized (Glas-Potter) in 3 vol of cold deionized water. The homogenate was centrifuged at 12,000 rpm at 0–4 °C for 30 min. Saturated ammonium sulfate solution was added to the supernatant fraction to form a 40% solution, which was stirred for 30 min at 0–4 °C and then centrifuged at 12,000 rpm for 15 min. Following this same procedure, the recovered supernatant was subsequently fractionated with saturated ammonium sulfate solution using first a 50%, and then a 75% salt saturation. The precipitate recovered from the 75% saturated fraction, possessing ALR2 activity, was redissolved in 0.05 M NaCl and dialyzed overnight in 0.05 M NaCl. The dialyzed material was used for the enzymatic assay.

5.2.2.2. Aldehyde reductase (ALR1). Rat kidney ALR1 was prepared in accordance with a previously reported method.²² Kidneys were quickly removed from rats following euthanasia and homogenized (Glas-Potter) in 3 vol of 10 mM sodium phosphate buffer, pH = 7.2, containing 0.25 M sucrose, 2.0 mM EDTA dipotassium salt and 2.5 mM β-mercaptoethanol. The homogenate was centrifuged at 12,000 rpm at 0–4 °C for 30 min and the supernatant was subjected to a 40–75% ammonium sulfate fractionation, following the same procedure previously described for ALR2. The precipitate obtained from the 75% ammonium sulfate saturation, possessing ALR1 activity, was redissolved in 50 vol of 10 mM sodium phosphate buffer, pH = 7.2, containing 2.0 mM EDTA dipotassium salt and 2.0 mM β-mercaptoethanol and dialyzed overnight using the same buffer. The dialyzed material was used in the enzymatic assay.

5.2.3. Enzymatic assays. The activity of the four test enzymes was determined spectrophotometrically by monitoring the change in absorbance at 340 nm, which is due to the oxidation of NADPH or the reduction of NAD⁺ catalyzed by ALR2, ALR1 and GR or SD, respectively. The change in pyridine coenzyme concentration/min was determined using a Beckman DU-64 kinetics software program (Solf Pack TM Module).

ALR2 activity was assayed at 30 °C in a reaction mixture containing 0.25 mL of 10 mM D,L-glyceraldehyde, 0.25 mL of 0.104 mM NADPH, 0.25 mL of 0.1 M sodium phosphate buffer (pH = 6.2), 0.1 mL of enzyme extract and 0.15 mL of deionized water in a total volume of 1 mL. All the above reagents, except D,L-glyceraldehyde, were incubated at 30 °C for 10 min; the substrate was then added to start the reaction, which was monitored for 5 min. Enzyme activity was calibrated by diluting the enzymatic solution in order to obtain an average

reaction rate of 0.011 ± 0.0010 absorbance units/min for the sample.

ALR1 activity was determined at 37°C in a reaction mixture containing 0.25 mL of 20 mM sodium D-glucuronate, 0.25 mL of 0.12 mM NADPH, 0.25 mL of dialyzed enzymatic solution and 0.25 mL of 0.1 M sodium phosphate buffer (pH = 7.2) in a total volume of 1 mL. The enzyme activity was calibrated by diluting the dialyzed enzymatic solution in order to obtain an average reaction rate of 0.015 ± 0.0010 absorbance/min for the sample.

SD activity²¹ was determined at 37°C in a reaction mixture containing 0.25 mL of 10 mM sorbitol, 0.25 mL of 0.47 mM NAD⁺, 0.25 mL of 3.75 mU/mL enzymatic solution and 0.25 mL of 100 mM Tris/HCl buffer (pH = 8) in a total volume of 1 mL. All the reagents were incubated at 37°C for 1 min, after which the reaction was monitored for 3 min.

GR activity²³ was determined at 37°C in a mixture containing 0.25 mL of 1 mM glutathione disulfide, 0.25 mL of 0.36 mM NADPH, 0.25 mL of 4.5 mU/mL enzymatic solution and 0.25 mL of 0.125 sodium phosphate buffer (pH = 7.4) supplemented with 6.3 mM EDTA potassium salt, in a total volume of 1 mL.

5.2.4. Enzymatic inhibition. The inhibitory activity of the newly synthesized compounds against ALR2, ALR1, SD and GR was assayed by adding 0.1 mL of the inhibitor solution to the reaction mixture described above. All the inhibitors were dissolved in water and the solubility was facilitated by adjustment to a favourable pH. After complete dissolution, the pH was readjusted to 7. To correct for the nonenzymatic oxidation of NADPH or reduction of NAD⁺ and for the absorption by the compounds tested, a reference blank containing all the above assay components except the substrate was prepared. The inhibitory effect of the new derivatives was routinely estimated at a concentration of 10^{-4} M. Those compounds found to be active were tested at additional concentrations between 10^{-5} and 10^{-7} M. The determination of the IC₅₀ values was performed by using linear regression analysis of the log-dose–response curve, which was generated using at least four concentrations of the inhibitor causing an inhibition between 20% and 80%, with two replicates at each concentration. The 95% confidence limits (95% CL) were calculated from *t* values for *n* – 2, where *n* is the total number of determinations.

5.3. Pharmacology

5.3.1. Materials and methods. Experiments were carried out using Sprague Dawley albino rats, 45–55 g b.w., supplied by Harlan-Nossan, Italy. Animal care and treatment conformed to the ARVO Resolution on the Use of Animals in Ophthalmic and Vision Research. The galactose diet consisted of a pulverized mixture of 50% D-galactose and 50% TRM laboratory chow (Harlan Teckland, UK), and the control diet consisted of normal

TRM. Both control and experimental rats had access to food and water ad libitum.

5.3.2. Prevention of cataract development. Animals were randomly divided into groups of equal average body weight with 15 rats per group. The test compounds **3** and tolrestat were administered four times daily as eye-drops of appropriate concentrations. The vehicle in which ARIs were contained was administered with the same dose regimen to the control group, which was given access to the galactose diet, and to the group fed with a normal diet, which was included to record the aspect of normal lenses. Groups treated with the tested compounds were pre-dosed 1 day before switching their diet to galactose-containing chow.

Lenses were examined using slit-lamp microscopy, after dilating the pupils with atropine 1% Farmigela, Italy, in order to establish their status of integrity.

Nuclear cataracts, which appeared as a pronounced central opacity readily visible as a white spot, were evaluated. The number of animals which attained this stage was recorded, and the ability of the test compounds to prevent cataract development was assessed on the basis of comparison with galactosemic rats treated only with the vehicle.

5.4. Computational chemistry

Computations were performed using the software package Sybyl³² running on a Silicon Graphics R12000 workstation. A starting model of compound **3** was obtained by modifying a crystal structure retrieved from a search by substructures using the October 2002 release of the Cambridge Structural Database (refcode: DAF-FIZ). Geometry optimizations were achieved with the SYBYL/MAXIMIN2 minimizer by applying the BFGS (Broyden, Fletcher, Goldfarb and Shannon) algorithm and setting a root mean square gradient of the forces acting on each atom of 0.05 kcal/mol Å as the convergence criterion. The crystal structure of the ALR2/sorbitol complex reported at 2.3 Å resolution by Urzhumtsev et al.¹⁵ was used for docking experiments. Hydrogens were added to the unfilled valences of the amino acids according to standard geometries of the Tripos force field. Charges of the ALR2 atoms were calculated by the Kollman all-atom (Lys, Asp and Glu side chains were modelled in their ionized forms). Flexible docking was performed with FlexX²⁷ implemented in Sybyl. The evaluation function was based on the Tripos force field.³³

References and notes

1. Kador, P. F. *Med. Res. Rev.* **1988**, *8*, 325.
2. Tomlison, D. R.; Stevens, E. J.; Diemel, L. T. *Trends Pharmacol. Sci.* **1994**, *293*.
3. Ammon, H. P. T.; Häring, H. U.; Kellerer, M.; Laube, H.; Mosthaf, L.; Verspohl, E. J.; Wahl, M. A. *Adv. Drug Res.* **1996**, *27*, 171.
4. Ashizawa, N.; Tomoji, A. *Drugs Future* **1998**, *23*, 521.

5. Costantino, L.; Rastelli, G.; Vianello, P.; Cignarella, G.; Barlocco, D. *Med. Res. Rev.* **1999**, *19*, 3.
6. Sarges, R.; Oates, P. J. *Prog. Drug Res.* **1993**, *40*, 99.
7. Da Settimo, F.; Primofiore, G.; Da Settimo, A.; La Motta, C.; Taliani, S.; Simorini, F.; Novellino, E.; Greco, G.; Lavecchia, A.; Boldrini, E. *J. Med. Chem.* **2001**, *44*, 4359.
8. Da Settimo, F.; Primofiore, G.; Da Settimo, A.; La Motta, C.; Simorini, F.; Novellino, E.; Greco, G.; Lavecchia, A.; Boldrini, E. *J. Med. Chem.* **2003**, *46*, 1419.
9. Banditelli, S.; Boldrini, E.; Vilaro, G. P.; Cecconi, I.; Cappiello, M.; Dal Monte, M.; Marini, I.; Del Corso, A.; Mura, U. *Exp. Eye Res.* **1999**, *69*, 533.
10. Sarges, R.; Schnur, R. C.; Belletire, J. L.; Peterson, M. J. *J. Med. Chem.* **1988**, *31*, 230.
11. Sarges, R.; Goldstein, S. W.; Welch, W. M.; Swindell, A. C.; Siegel, T. W.; Beyer, T. A. *J. Med. Chem.* **1990**, *33*, 1859.
12. Da Settimo, A.; Marini, A. M.; Primofiore, G.; Da Settimo, F.; Salerno, S.; La Motta, C.; Pardi, G.; Ferrarini, P. L.; Mori, C. *J. Heterocycl. Chem.* **2000**, *37*, 379.
13. Ferrarini, P. L.; Mori, C.; Badawneh, M.; Calderone, V.; Greco, R.; Manera, C.; Martinelli, A.; Nieri, P.; Saccomanni, G. *Eur. J. Med. Chem.* **2000**, *35*, 815.
14. Da Settimo, A.; Marini, A. M.; Primofiore, G.; Da Settimo, F.; Salerno, S.; Simorini, F.; Pardi, G.; La Motta, C.; Bertini, D. *J. Heterocycl. Chem.* **2002**, *39*, 1001.
15. Urzhumtsev, A.; Tête-Favier, F.; Mitschler, A.; Barban-ton, J.; Barth, P.; Urzhumtseva, L.; Biellmann, J. F.; Podjarny, A. D.; Moras, D. *Structure* **1997**, *5*, 601.
16. Ware, E. *Chem. Rev.* **1950**, *46*, 403.
17. De Ruiter, J.; Brubaker, A. N.; Garner, M. A.; Barksdale, J. M.; Mayfield, C. A. *J. Pharm. Sci.* **1987**, *76*, 149.
18. Mayfield, C. A.; De Ruiter, J. *J. Med. Chem.* **1987**, *30*, 1595.
19. Müller, P.; Hockwin, O.; Ohrloff, C. *Ophthalmic Res.* **1985**, *17*, 115.
20. Hockwin, O.; Müller, P.; Krolczyk, J.; McCue, B. A.; Mayer, P. R. *Ophthalmic Res.* **1989**, *21*, 285.
21. Lindstad, R. I.; Hermansen, L. F.; Mc Kinley-Mc Kee, J. S. *Eur. J. Biochem.* **1994**, *221*, 847.
22. Ward, W. H. J.; Sennitt, C. M.; Ross, H.; Dingle, A.; Timmus, D.; Mirless, D. J.; Tuffin, D. P. *Biochem. Pharmacol.* **1990**, *39*, 337.
23. Fitzgerald, G. B.; Bauman, C.; Hussoin, M. S.; Wick, M. M. *Biochem. Pharmacol.* **1991**, *41*, 185.
24. Hu, T.; Merola, L. O.; Kuwabara, T.; Kinoshita, J. H. *Invest. Ophthalmol. Vis. Sci.* **1984**, *25*, 603.
25. Sestan, K.; Bellini, F.; Fung, S.; Abraham, N.; Treas-urywala, A.; Humber, L.; Simard-Duquesne, N.; Dvornik, D. *J. Med. Chem.* **1984**, *27*, 255.
26. Chaudhry, P. S.; Cabrera, J.; Juliani, H. R.; Varma, S. D. *Biochem. Pharmacol.* **1983**, *32*, 1995.
27. Rarey, M.; Kramer, B.; Lengauer, T.; Klebe, G. *J. Mol. Biol.* **1996**, *261*, 470.
28. Bernstein, F. C.; Koetzle, T. F.; Williams, G. J. B.; Meyer, E. F., Jr.; Brice, M. D.; Rodgers, J. R.; Kennard, O.; Shimanouchi, T.; Tasumi, T. *J. Mol. Biol.* **1977**, *112*, 535.
29. Database searching (SWISS-PROT), sequence alignment and analysis of rat and pig ALR2 sequences were carried out using FASTA (Pearson, W. R. *Proc. Natl. Acad. Sci. U.S.A.* **1988**, *85*, 2444); and BLAST programs (Wang, S.; Pak, Y. *J. Phys. Chem. B* **2000**, *104*, 354). The SWISS-PROT accession numbers for rat and pig ALR2 types are P07943 and P80276, respectively.
30. Wilson, D. K.; Tarle, I.; Petrash, J. M.; Quirocho, F. A. *Proc. Natl. Acad. Sci. U.S.A.* **1993**, *90*, 9847.
31. Hayman, S.; Kinoshita, J. H. *J. Biol. Chem.* **1965**, *240*, 877.
32. *Sybyl Molecular Modelling* (version 6.8); Tripos: St. Louis, MO.
33. Vinter, J. G.; Davis, A.; Saunders, M. R. *J. Comput. Aided Mol. Des.* **1987**, *1*, 31.
34. CLOGP ver. 2.0, BioByte Corp., Claremont, CA.